

CNRS  
*Centre National de la Recherche Scientifique*

INFN  
*Istituto Nazionale di Fisica Nucleare*



## **Automatic Alignment system during the second science run of the Virgo interferometer**

VIR-0645B-10

M. Mantovani

*Issue:* 1

*Date:* December 13, 2011

VIRGO \* A joint CNRS-INFN Project  
Via E. Amaldi, I-56021 S. Stefano a Macerata - Cascina (Pisa)  
Secretariat: Telephone (39) 050 752 521 \* FAX (39) 050 752 550 \* Email W3@virgo.infn.it

## Contents

<b>1</b>	<b>The Virgo gravitational wave detector</b>	<b>2</b>
<b>2</b>	<b>Angular control system</b>	<b>3</b>
<b>3</b>	<b>Automatic Alignment control scheme</b>	<b>4</b>
3.1	Control Configuration . . . . .	5
<b>4</b>	<b>Performances</b>	<b>6</b>
<b>5</b>	<b>Conclusions</b>	<b>7</b>
<b>6</b>	<b>Acknowledgements</b>	<b>8</b>

---

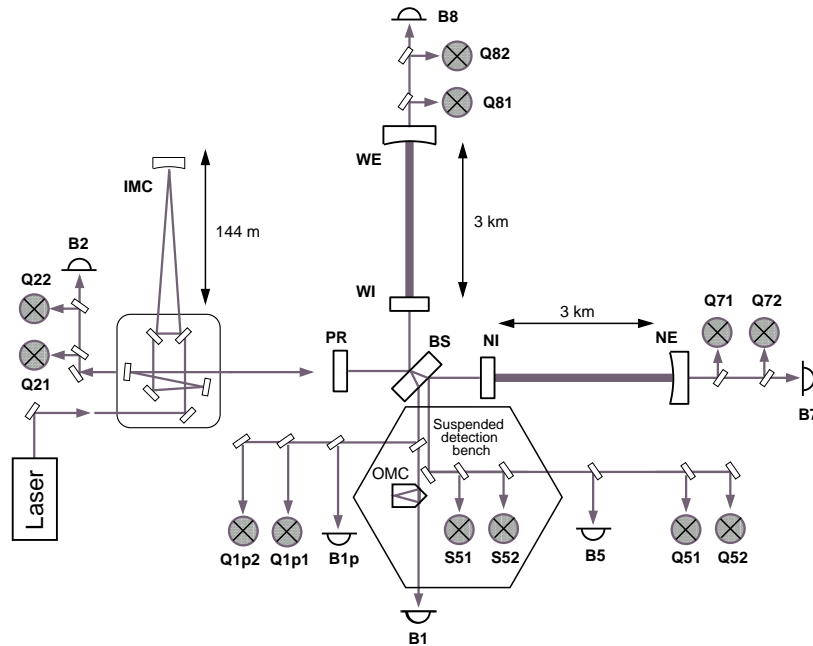


Figure 1: Simplified scheme of the Virgo optical design. The diodes, placed on external detection benches, used for longitudinal (with names starting with **B**), and angular control (starting with **Q**) are shown. On the suspended detection bench two more quadrant diodes used for angular control (with names starting with **S**) are placed. PR is the power recycling mirror, BS is the beam splitter, NI and NE are the input and end mirrors of the North cavity (equally for the West cavity). IMC and OMC are the input and output mode cleaners, respectively. See main text for details.

### Abstract

In this paper the performances of the Automatic Alignment sensing and control system in the Virgo gravitational wave detector, during the second scientific run from July 7<sup>th</sup> 2009 to January 8<sup>th</sup> 2010, are described. The accuracy of the angular control loops fulfills the original Virgo requirements, reaching the accuracy of a few nano-radians for the most critical angular degrees of freedom, and the control noise is below the Virgo design sensitivity in the whole detection band.

## 1 The Virgo gravitational wave detector

The Virgo interferometer [1] is a ground based gravitational wave detector consisting of a Michelson interferometer with 3 km long Fabry-Perot cavities in its arms and a power-recycling mirror, see Figure 1. The main optical elements are fused silica cylinders suspended in ultra-high vacuum by a seismic isolation system, *super-attenuators* [2]. This suspension system provides an excellent seismic isolation in the frequency range above the resonances of the mechanical system in the vertical and horizontal directions (more than 10 orders of magnitude above a few Hz). The *super-attenuator* is composed of an inverted pendulum, with a very low mechanical resonant frequency, which provides a pre-isolation stage, and a cascade of attenuator filters.

The last stage of the suspension is formed by the *marionette* and the *reference mass*. The marionette, which is a massive element connected to the last vertical isolation stage, supports the reference mass and the mirror and acts on their position by means of four steel wires, in the longitudinal and in the angular degrees of freedom. The reference mass is a cylindrical component which surrounds the mirror and acts on its position by coil-magnet actuators.

The input beam is generated by a system of master/slave lasers with a power of 60 W and a wavelength of 1064 nm. The beam jitter is reduced by passing the input light through a 144 m long *input mode-cleaner* (IMC). The laser beam is split at the *beam splitter* mirror (BS) into two beams which are injected into the two orthog-

onal Fabry-Perot arm cavities (North and West arms), to enhance the phase shift produced by the optical path length variation of the beam caused by a gravitational wave.

The longitudinal positions of all the mirrors are controlled in such a way that the arm cavities are resonant and the recombination of the beams at the BS creates a destructive interference in the main output port (B1), the asymmetric port, see Figure 1.

This is the *dark fringe* condition. In this condition almost all the light is reflected back to the power recycling mirror (PR), only a millionth part of the light circulating in the cavities reaches the dark fringe. The presence of this mirror allows to increase the circulating power in the interferometer.

The light coming from the dark port of the interferometer is filtered by an *output mode cleaner* (OMC), before being detected by a set of high-sensitivity photo-diodes at the B1 detection port.

## 2 Angular control system

The detection principle of a gravitational wave interferometer is to sense the passage of a gravitational wave as a change in the intensity of light at the asymmetric port, due to the phase shift in the long arms. This is possible only if the test masses are suspended well enough to be considered as *free-falling test masses*.

These instruments provide a useful signal only when the optical components are positioned precisely at predefined locations relative to each other. This set of positions is called the *operating point*. Sophisticated electro-optical feed-back control systems are required to continuously measure and restore the operating point. A misalignment or a displacement of a mirror produces a variation of the effective arm length of the interferometer which can mimic the effect of a gravitational wave. For this reason two separate systems to control the mirror position are used: one for the longitudinal position along the optical axis (called *Locking*), and the other for the alignment (called *Automatic Alignment*).

In order to reach the design strain sensitivity of Virgo,  $h < 3 \cdot 10^{-21}/\sqrt{\text{Hz}}$  at 10 Hz, the position of the mirrors has to be actively maintained at the *operating point* with very high accuracy. Tolerable deviations from the operating point along the optical axis are typically of the order of  $\sim 10^{-15} - 10^{-12}$  m in the longitudinal direction [3] and  $\sim 10^{-1} - 10^{-3}$   $\mu\text{rad}$  of total RMS [4] in the angular directions, while the free motion of the suspended mirrors would be orders of magnitude larger than that: from 10 to 1  $\mu\text{rad}$  in the region between 100 mHz and a few Hz.

Thus the angular control system has to be implemented in order to reduce the mirror misalignments in the frequency region in which the super-attenuator does not fulfill the alignment requirements, below the mechanical resonances (a few Hz).

During the switch-on procedure of the longitudinal control loops (called also *lock*), the angular positions of the main mirrors and of the beam splitter are controlled by using local references (*Local Control* [5], with a stability of some  $\mu\text{rad}$  per hour).

The mirror angular positions in data taking mode can not be controlled by the Local Controls due to the long term drifts of the references and low accuracy of the controls, which spoils the overall alignment, and due to the high electronic/shot noise of the sensors used.

After the lock has been acquired the angular control is switched to a global control system, the *Automatic Alignment*, which uses error signals coming from the interferometer itself with a modulation-demodulation technique. The Automatic Alignment is a servo-loop system designed to reduce the fluctuations of the mirror angular positions with respect to the beam, to maintain the overall alignment of the optical elements and to reduce the noise at the dark fringe port (the local control sensing noise is more than  $10^{-4}$   $\mu\text{rad}/\sqrt{\text{Hz}}$ , as opposed to the global sensing noise of about  $10^{-6} - 10^{-7}$   $\mu\text{rad}/\sqrt{\text{Hz}}$ ).

The Automatic Alignment system controls the angular pitch and yaw<sup>1</sup> misalignments of the seven degrees of freedom, namely the PR, BS, NI, WI, Differential End ( $\frac{\theta_{\text{WE}} - \theta_{\text{NE}}}{2}$ ) and Common End ( $\frac{\theta_{\text{WE}} + \theta_{\text{NE}}}{2}$ ), and the main input beam (IB). The alignment error signals are extracted using five beams coming out of the interferome-

<sup>1</sup>The pitch and yaw directions are defined as the rotation around the horizontal ( $x$ ) and vertical ( $y$ ) axis respectively, where the  $z$  axis is defined along the beam.

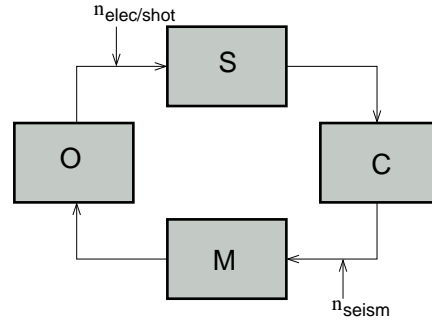


Figure 2: Blocks scheme for the angular control system. The *Sensing* composed by the readout electronics (quadrant diodes, demodulators and ADC) labeled with **S**; the *Control*, formed by the control matrix and the corrector filters, labeled with **C**; the *Mechanics*, the mechanical Transfer Function (TF) from the correction injection point and the angular displacement of the optics, labeled with **M**; and the *Optical configuration*, which takes into account the TF between the mirror angular displacement and the optical signals, labeled with **O**. The main sources of noise in the angular control scheme are the seismic noise  $n_{seism}$  and the sensing electronic/shot noise  $n_{elec/shot}$ .

ter. They are: the main beam reflected by the interferometer (Q2), the two beams transmitted by the long arm cavities (Q7/8), the pick-off beam at the secondary surface of the BS (Q5 for the quadrants in air on the detection bench and S5 for the quadrants suspended in vacuum) and the beam detected in the asymmetric port before the OMC (Q1p). At each detection port two quadrant diodes (*quadrants* for short) are installed at 90 deg of Gouy phase difference to have independent signals, see Figure 1. These are photo-diodes with 4 separate elements. Each quadrant diode can provide four signals: the sum over four quadrants gives the same signal as a normal photo-diode. The differences between the upper and lower elements and the left and right elements are computed and give the absolute vertical and horizontal positions of the beam on the diode, *DC signals*. Demodulation of the differential quadrant diode outputs at the modulation frequency yields two additional signals (in-phase and quadrature) that contain information about the angle and position (vertical and horizontal respectively) of the phase front of the carrier with respect to the sideband, *RF signals*.

### 3 Automatic Alignment control scheme

The angular control scheme can be described with a block diagram, as it is shown in Figure 2:

The *Sensing* (**S**) which is formed by the sensing electronics: quadrant diodes and readout electronics, which detect the interferometer beams to extract the informations about mirror misalignments.

The *Control* (**C**) which is formed by the *Control Matrix* and the *Correctors*. The control matrix gives the relation between the set of quadrant signals and the set of mirror tilts; its entries are the low frequency limit, below the cavity pole, of the transfer functions between the angular degrees of freedom and the quadrant signals [6], sampled at 2 kHz.

The angular corrections are constructed by filtering the error signals with properly designed control filters (correctors).

The *Mechanics* (**M**) which corresponds to the Transfer Function from the marionetta, where the angular corrections are applied, to the mirror angular displacement.

The *Optical configuration* (**O**) which represents the interferometer response to the mirror misalignments.

The main sources of noise in the angular control scheme are the *Seismic noise*,  $n_{seism}$ , which dominates the error signals below some Hz, and the *Electronics/Shot noise* of the sensing path,  $n_{elec/shot}$ , which dominates the error signals above 10 Hz. The aim of the Automatic Alignment system is to suppress the seismic displacement of the optics, at low frequency, while cutting off the electronic noise for not reintroducing it in the gravitational wave signal, starting from 10 Hz.

For the Automatic Alignment system two topologies of control have been developed: the *Fast control* and the

### *Drift control.*

The Fast control uses the global signals with a control bandwidth of a few Hz, where all the local controls are switched off.

The Drift control is a mixture of a global and local controls; the overall alignment is kept by a low frequency global control, with a few mHz of bandwidth, while the high frequency control is done by using local references; this avoids the slow independent drifts of the mirrors and allows maintaining a reasonably good global alignment that would not occur with local control alone.

In a perfectly decoupled control system all the angular degrees of freedom should be controlled by a fast control mode, but in reality strong couplings between the degrees of freedom are present. A way to separate them is to implement an hierarchical control engaging the controls with different bandwidths: the dominant degrees of freedom should be engaged with a larger control bandwidth to reduce their influence on the other degrees of freedom (d.o.f.).

Moreover, the choice between fast and drift control depends also on noise issues. For example, if a given d.o.f. has a strong coupling factor to the dark fringe, it is necessary to engage it with a fast control topology in order to have a larger control bandwidth, thus more accuracy, and a less noisy control (since the *local control system*, which has much higher electronic noise, is switched off); on the other hand if the error signal which senses that d.o.f. is noisy and the coupling factor into dark fringe is low it is sufficient and advisable to engage that d.o.f. with a drift control since the narrow frequency band of the control helps in the decoupling of the d.o.f. from the dominant ones <sup>2</sup>.

The design of the control filters for the fast control mode is a very important issue since the low frequency part, below the unitary gain frequency, determines the accuracy of the loop, and the high frequency part determines the noise performance of the loop. The control filter is developed starting from the modeling of the super-attenuator transfer function, from actuator to mirror, which is essentially a double pendulum with resonance frequencies at a few Hz. The control filters have to be designed in order to suppress the mechanical resonances of the suspension and to have a large low frequency gain.

## 3.1 Control Configuration

The angular control system is formed by a complete set of RF error signals used for aligning the mirrors with respect to the beam, plus some reference error signals used to define the beam plane of the interferometer, see Figure 3. The beam plane has to be defined by pointing the beam on absolute references in three points, by using three angular d.o.f. to fix the beam to the references, while the remaining d.o.f. will be aligned with respect to the beam. The plane of the interferometer was defined using the input mirrors and the Common End d.o.f.

The input mirrors are controlled so that the beam hits the center of the arm cavity terminal mirrors. The error signal is generated by injecting a sinusoidal excitation to the terminal mirrors (with frequencies below the detection range, from 6 to 8 Hz) and evaluating the longitudinal/angular coupling. If the beam is not well centered on the mirrors, the sinusoidal excitation will be present also in the longitudinal error signals. The continuous centering servo, with a bandwidth of  $\sim$ mHz, applies misalignment corrections to the input mirrors in order to steer the beam on the terminal mirrors and minimize the angular/longitudinal coupling at the excitation frequency, which reduces also the control noise of the arm cavity mirrors.

The Common End alignment is controlled in *fast control mode* by using the DC signal of the suspended quadrant at the BS pick-off (S51).

Most of the quadrant diodes are placed on external detection benches since the environmental noises do not couple strongly to the RF signals <sup>3</sup>, as they measure the beat between the sidebands and the carrier. This is not true for the DC signals, which detect the relative position of the quadrant diode with respect to the beam. For this reason in order to have a clean error signal, the environmental noise has to be suppressed by suspending

<sup>2</sup>For example the Input Beam has been controlled in drift control mode, as it will shown in the next section, since the Input Beam error signal is strongly affected by the Common End mode and since its coupling in the sensitivity is very low.

<sup>3</sup>It has been experienced that the air currents spoil the error signals at low frequency, below  $\sim$ 1 Hz, but the installation of plexiglass covers on the benches strongly reduced the effect.

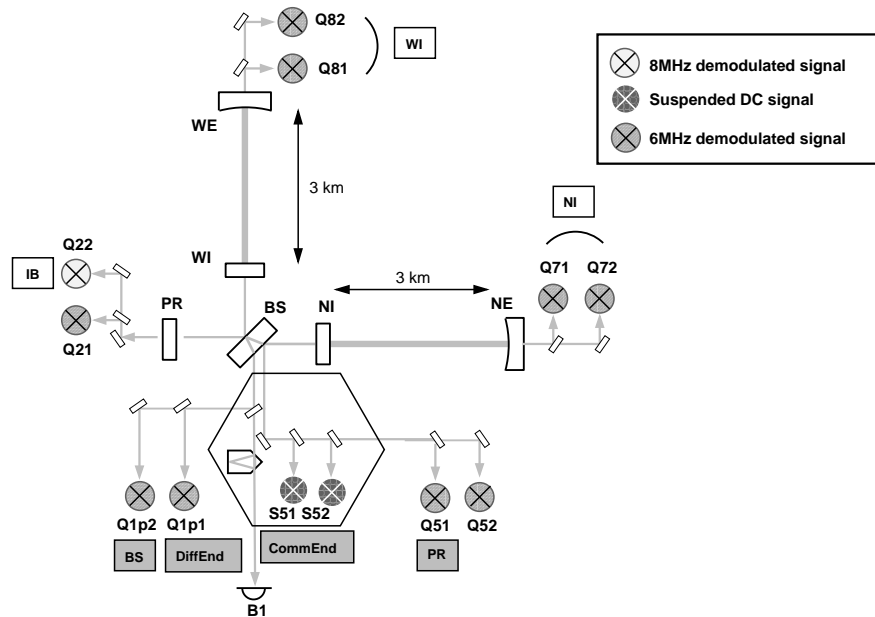


Figure 3: Configuration of the Automatic Alignment control scheme for the science run VSR2. The schematic shows the signals used to control each d.o.f. (labeled in a grey or white box). The degrees of freedom labeled in gray are controlled by using a fast control topology while the white ones are controlled in drift control mode. For example the Differential End mode is controlled by using the Q1p1 quadrant signal in fast control mode (for the Differential End mode the error signal is extracted at the asymmetric port before the OMC in order to not suppress the higher order modes content) demodulated at  $\sim 6$  MHz.

the quadrant in vacuum.

After the plane is defined, the remaining angular degrees of freedom have to be aligned with respect to the main beam. For the angular control two modulation frequencies are used:  $\sim 6$  MHz, which is resonating in the central interferometer, and  $\sim 8$  MHz which does not enter in the interferometer.

The input beam (IB) is controlled in drift control mode by using the RF signal, demodulated at 8 MHz, reflected by the interferometer (Q22). The two quadrants placed at the dark port, Q1p1 and Q1p2 separated by 90 deg of Gouy phase, demodulated at 6 MHz, are used to control, in fast control mode, the Differential End and the BS angular displacements.

At last the PR mirror is controlled by using the pick-off beam of the BS mirror demodulated at 6 MHz (Q51) in fast control mode.

## 4 Performances

The angular control for the Virgo detector was completed in the commissioning period between winter 2004 and the beginning of 2007 [6]; all the angular degrees of freedom were globally controlled, with a *fast* or *drift* control mode, depending on the noise performance of each loop.

The quality of an angular control can be evaluated by: the robustness; the accuracy, thus the total RMS of the mirror angular displacements; and by the control noise performances, corresponding to the noise re-injected to the gravitational wave signal in the detection band (above 10 Hz).

During the first Virgo science run (VSR1) the angular control system was very robust, allowing a duty cycle of more than 80 % with the longest locking period of about 94 h. The accuracy of the loops was compliant with the requirements, but the control noise was above the design sensitivity below 20 Hz [4].

From July 7<sup>th</sup> 2009 to January 2010 the second Virgo science run (VSR2) in coincidence with the two LIGO detectors (HLO in Hanford, WA and LLO in Livingstone, LA - USA each [7]) took place.

The interferometer configuration was improved with respect the first scientific run by increasing the input power from 8 to 17 W to improve the shot noise. A Thermal Compensation System (TCS) was then implemented to reduce the thermal lensing on the input mirrors [8].

The stability and robustness of the Virgo detector was very high, achieving a duty cycle of more than 80% with the longest locking period of 143 h allowing to have: more than 90% of duty cycle for single detector, more than 50% for double coincidence and about 20% for triple coincidence [9]. The duty cycle was mainly limited by maintenance and commissioning periods <sup>4</sup>.

From the point of view of the angular control system, since the accuracy requirements were already fulfilled for VSR1 <sup>5</sup>, the commissioning of the automatic alignment system in the period between the two runs was focused to reduce the angular control noise.

Since the unity gain frequency of the fast angular controls is of the order of a few Hz, the noise performance depends on the dark fringe coupling factor, on the high frequency roll-off of the control filters and on the sensing noise (electronic plus shot noise).

In order to reduce the angular control noise contribution to the Virgo sensitivity some improvements to the Automatic Alignment control scheme have been applied.

The sensing noise has been lowered thanks to the implementation of more performing demodulator and ADC (analog-digital converter) boards. The new demodulator boards have a lower electronic noise, smaller than the ADC noise, and remotely tunable gain to optimize the signal amplitude at each locking phase. The new ADC boards have smaller non-linearities, with respect to the ones used in VSR1, even if their noise is still dominant for the most critical d.o.f., such as the Differential End and Common End modes.

Rigid plexiglass covers have been installed on the detection benches to reduce the environmental noise, reducing the air currents which affect the error signals in the low frequency region (below a few Hz) spoiling the control accuracy.

Moreover some modifications in the control strategy have been applied, as the use of a second quadrant on the dark fringe beam <sup>6</sup> to sense the BS and the use of the suspended quadrant diode for the Common End mode. Both of these signals have better performances in terms of electronics/shot noise and are less affected by environmental noises.

As a result during VSR2 the angular control noise was below the design sensitivity in the entire detection band, see Figure 4.

## 5 Conclusions

During the second Virgo scientific run the angular control was complete, robust and well performing in terms of accuracy and control noise reintroduction in the gravitational wave signals.

The noise performances, with respect to VSR1, were optimized by improving the electronics and the control strategy with respect to the VSR1 scheme, resulting in a control noise below the design sensitivity in the whole detection band.

The system is currently in commissioning phase to fulfill the requirements for the Virgo+ configuration, for the third Virgo scientific run (VSR3) which should start at the end of July 2010, which requires better performances in the 10 Hz region. The angular control will be modified to face with the Monolithic Suspensions implementation, whose installation is foreseen at the beginning of 2010, and further improvements on the electronics are planned.

---

<sup>4</sup>The evaluations on the duty cycle and the coincidence periods have been done by simply taking into account the science mode periods for all the three detectors.

<sup>5</sup>The accuracy of the control loops were fulfilling the requirements, being of the order of the nrad for Differential and Common End modes and tens of nrad for the central interferometer d.o.f

<sup>6</sup>The second quadrant on the dark fringe (Q1p2) is at 90 deg of Gouy phase difference with respect to the quadrant used to sense the Differential End mode



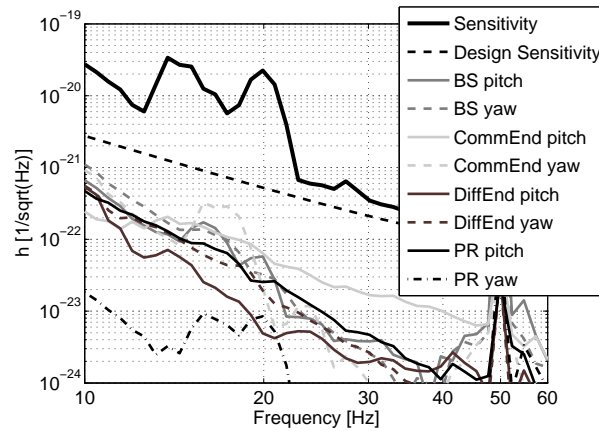


Figure 4: Noise budget of the Automatic Alignment control system during VSR2 compared to the design sensitivity curve and to the measured sensitivity. The total angular noise is well below the sensitivity curve and below the Virgo design in the whole detection band.

## 6 Acknowledgements

This research activity has been partially supported by Regione Toscana (Italy) through the program POR CreO FSE 2007-2013 of the European Community, within the project n. 18113 (ISAV).

## References

- [1] T. Accadia *et al.*, “Status And Perspectives Of The Virgo Gravitational Wave Detector”, J. Phys. Conf. Ser. 203, 012074 (2010). **2**
- [2] F. Acernese *et al.* “Measurements of Superattenuator seismic isolation by Virgo interferometer”, Astroparticle Physics 33 (2010) 182-189 **2**
- [3] F. Acernese *et al.* [Virgo Collaboration], “Lock acquisition of the Virgo gravitational wave detector”, doi:10.1016/j.astropartphys.2008.06.005 **3**
- [4] F. Acernese *et al.* “Automatic alignment for the first science run of the Virgo interferometer”, Astropart. Phys. 33, 131 (2010) **3, 6**
- [5] F. Acernese *et al.* [Virgo Collaboration], “A local control system for the test masses of the VIRGO gravitational wave detector”, *Astrop. Phys.* **20** (2004) 617-628 **3**
- [6] F. Acernese *et al.* [Virgo Collaboration], “The Virgo automatic alignment system”, *Class. Quant. Grav.* **23** (2006) S91-S102. **4, 6**
- [7] J. R. Smith *et al.* [LIGO Scientific Collaboration], “The path to the enhanced and advanced LIGO gravitational-wave detectors”, *Class. Quant. Grav.* 26 (2009) 114013 **6**
- [8] T. Accadia *et al.* [Virgo collaboration], “A Thermal Compensation System for the gravitational wave detector Virgo”, proceedings of the 12th Marcel Grossmann meeting. **7**
- [9] evaluations done by B. Swinkels and  
 ”<http://wwwcascina.virgo.infn.it/MonitoringWeb/Inspiral/index.html>” **7**